Supporting Information

Polyoxometalate-based Catalysts for Visible-Light Driven Hydrolytic Hydrogen Production: Coordinatively Unsaturated Cu-based Active Sites Enhance Performance

Quan-Quan Wang[†‡], Rong-Xian Ren[†‡], Rui-Jie Gong[†], Shao-Da Zhao[†], Pin-Fang Yan[†], and Yan Xu*[,†]

[†]College of Chemical Engineering, State Key Laboratory of Materials-Oriented Chemical Engineering, Nanjing Tech University, Nanjing 211816, P. R. China.

Experimental Section

Materials and Methods

All chemical reagents were purchased in Shanghai Aladdin without furthermore purification.

X-Ray crystallographic study

Select crystals with no impurities, no cracks, transparent and glossy surface under high power microscope. At 296 K, crystal data was collected by using Bruker Apex II CCD diffractometer with Mo Kα radiation (λ = 0.071073 nm). The structures were solved by utilizing direct method and refined by full-matrix least-squares methods with the SHELXL-2018/3 program package and restored the data. CCDC-2493449-2493450 contain the supplementary crystallographic data for **1** and **2**. These data can be obtained free of charge via www.ccdc.cam.ac.uk/data_request/cif, or by emailing data_request@ccdc.cam.ac.uk, or by contacting The Cambridge Crystallographic Data Centre, 12 Union Road, Cambridge CB2 1EZ, UK; fax: +44 1223 336033.

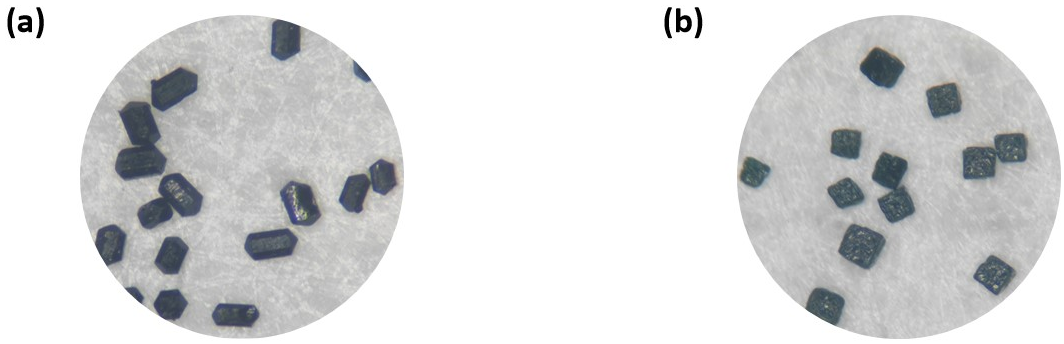

Figure. S1 (a) The crystal morphology of **1** and (b) **2**.

Table. S1 Crystallographic data of 1 and **2**.

Compound	**1**	**2**
Formula	$C_{72}H_{64}Cu_{8.50}N_2$ $_4NaO_{50}PW_{11.50}$	$C_{144}H_{162}Cu_{13}$ $N_{54}O_{66}SiW_{11}$
Formula weight	4773.79	6581.73
T (K)	193	296
Crystal system	Monoclinic	Trigonal
Space group	*C2/C*	*R-3*
a (Å)	28.447(3)	28.347(3)
b (Å)	12.6282(11)	28.347(3)
c (Å)	28.313(2)	19.755(5)

α (°)	90	90
β (°)	90.361(5)	90
γ (°)	90	120
V (Å^3)	10171.0(16)	13747(4)
Z	4	3
Dc (mg m^{-3})	3.118	2.385
μ (mm^{-1})	14.804	8.450
F (000)	8750	9411
Crystal size (mm^3)	0.12 × 0.11 × 0.10	0.13 × 0.12 × 0.12
radiation type	Mo Kα	Mo Kα
θ range (°)	1.764-25.005	1.323-25.024
Limiting indices	-33 ≤ h ≤ 33, -15 ≤ k ≤ 15, -33 ≤ l ≤ 33	-33 ≤ h ≤ 33, -33 ≤ k ≤ 33, -23 ≤ l ≤ 23
Reflections collected	64351	33122
R_{int}	0.0724	0.0799
Data/restraints/parameters	8944 / 42 / 788	5380 / 32 / 443
GOF	1.055	1.035
R_1[a], wR_2[b] [I>2σ(I)]	R_1 = 0.0914, wR_2 = 0.2568	R_1 = 0.0360, wR_2 = 0.0795
R_1[a], wR_2[b] (all data)	R_1 = 0.1118, wR_2 = 0.2708	R_1 = 0.0636, wR_2 = 0.0875

[a]$R_1 = \mathbf{\Sigma}||F_0| - |F_c||/\mathbf{\Sigma}|F_0|$. [b]w$R_2 = \mathbf{\Sigma}[w(F_0^2 - F_c^2)^2]/\mathbf{\Sigma}[w(F_0^2)^2]^{1/2}$.

PXRD and IR spectra of 1 and 2

The range of Fourier transform infrared (FTIR) spectra (KBr pellets) is from 4000 to 400 cm^{-1}. Nicolet Impact 410 Fourier transform infrared spectrometer was used for collecting the spectra. The IR spectra of compounds from 4000 to 400 cm^{-1} are shown in Figures. S2a, S2b. The compounds were ground to powder, mixed with KBr powder at a mass ratio of 1:150, then pressed into sheets, tested.

Powder X-ray diffraction (PXRD) patterns were collected on a Bruker D8X diffractometer with Cu Kα (λ = 0.15418 nm) radiation at 2θ in the range of 5-50°. The PXRD patterns of the compounds (Figures. S2c, S2d) were gathered under the ambient temperature. The experimental pattern is practical unanimity with the simulated result, confirming the phase purity of compounds.

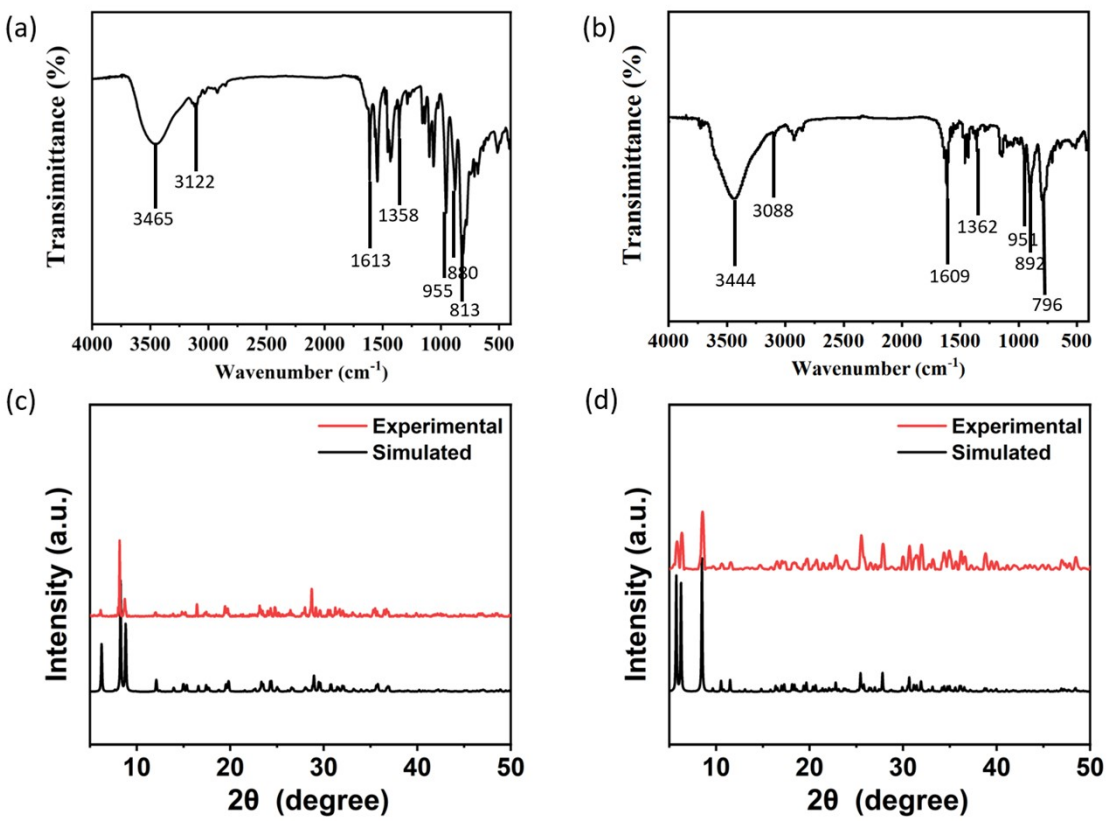

Figure. S2 (a) The IR spectra of **1** and (b) **2;** (c) the PXRD pattern of **1** and (d) **2**.

SEM and EDS mapping

The scanning electron microscopy (SEM) image of **1** and **2** are shown in Figure. S3. At the same time, the mapping images indicate that the distribution of elements on the compounds are uniform.

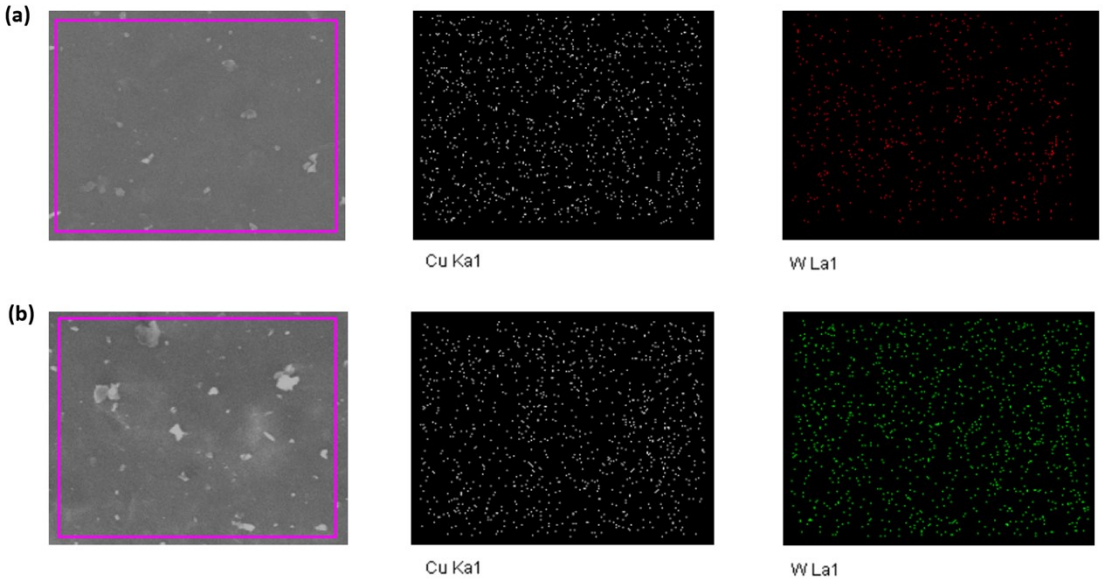

Figure. S3 (a) The SEM and EDS mapping images of **1**. (b) The SEM and EDS mapping images of **2**.

UV-vis analysis and Photoelectrochemical measurements

The range of ultraviolet-visible (UV-vis) is 200-800 nm. The reflectance spectra (reference: barium sulfate) were gathered on a Shimadzu UV-2600 spectrophotometer. Mott−Schottky plot was conducted were performed in an ambient environment through the electrochemical workstation (CHI 760e) in a standard three-electrode system: The carbon cloth (CC, 1 cm × 1 cm) modified with catalyst samples, carbon rod, and Ag/AgCl were used as the working electrode, counter electrode, and the reference electrode, respectively. The catalyst of 10 mg was ground to powder and then dispersed in 1 mL of 0.5% Nafion solvent by ultrasonication to form a homogeneous ink. Subsequently, 200 μL of the ink was deposited onto the carbon cloth and dried at room temperature for Mott-Schottky spots measurements. The Mott-Schottky plots were measured over an alternating current (AC) frequency of 1000 Hz, 1500 Hz, and 2000 Hz, and three electrodes were immersed in the 0.2 M Na_2SO_4 aqueous solution (pH=7). The light source and density were identical with that in the H_2 photoreduction experiments.

The Procedure of Photocatalytic HER

Devices

Figure. S4 The related equipment of photocatalytic HER.

The specific operation of photocatalytic HER

The specific photocatalytic performances of **1** and **2** were mainly estimated by the equipment (CEL-PAEM-D8, AULTT, China). A 300 W Xenon arc lamp (CEL-PF300-T8, AULTT, China) (photocurrent: 15 A) was the source of visible light. An external

condensate is used to eliminate heat from the Xenon arc lamp. Under its irradiation, the catalyst mixed with other reagents reacted in a Pyrex flask (100 mL). After the end of the reaction, the products were analyzed by performing gas chromatography (GC7920-TF2Z, AULTT, China). Finally, H_2 was detected by TCD.

Photocatalytic Performance in HER

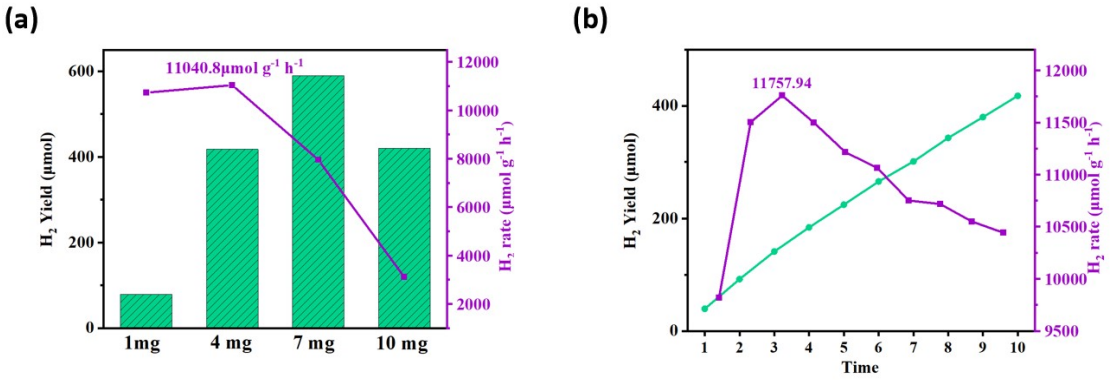

Figure. S5 (a) The effect of the amount of **2** on the yield of H_2; (b) H_2 yield and evolution rate as a function of time for 4 mg of **2**.

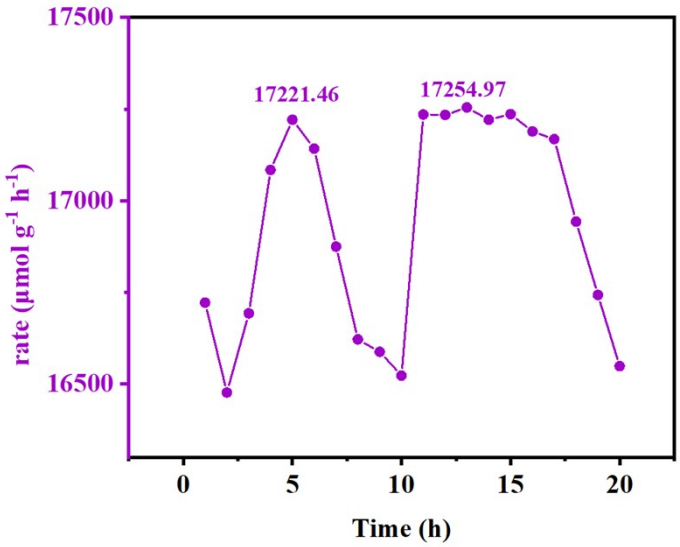

Figure. S6 The change in H_2 production rate of **1** after 10 hours of supplementation with PS and TEOA.

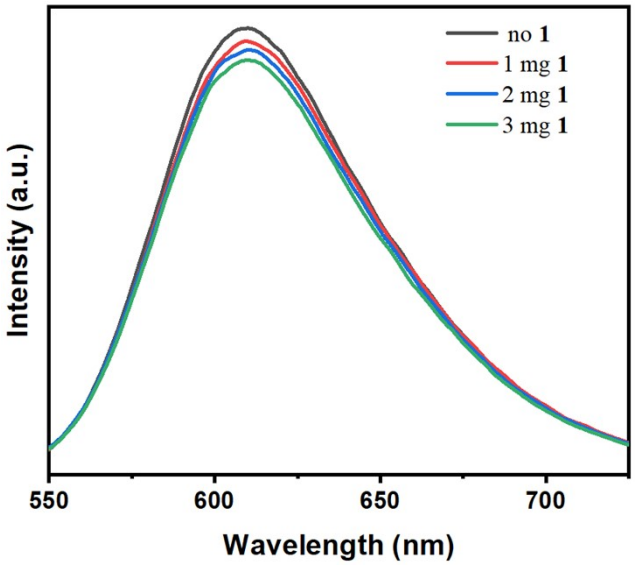

Figure. S7 Emission spectra of $[Ir(dtbbpy)(ppy)_2]PF_6$ in the presence of **1** at different concentrations.

The apparent quantum yield (AQY) for products was measured using the same photochemical experimental setup at 420, 550, 600 nm. The incident light density was measured using an ultraviolet radiation meter (FZ-A). The calculation of the apparent quantum yield was according to the following equations:

AQY = Ne/Np×100 %.

Ne= 2×number of evolved (H_2) molecules;

Np= the number of incident photons.

The AQYs for **Co-phen** and **Co-pzpy.**

Catalyst	**Incident light density ($mWcm^{-2}$)**	**AQY(%)**
1-420 nm	14.87	0.75
2-420 nm	14.74	0.87
1-550 nm	15.03	0.72
2-550 nm	14.78	0.79
1-600 nm	14.92	0.77

2-600 nm	14.43	0.83

Relevant Tables

Table S2 Bond lengths (Å) for **1**

W(1)-O(5)	1.696(13)	Cu(4)-O(7)	1.906(18)
W(1)-O(8)	1.861(16)	Cu(4)-O(3)	1.910(14)
W(1)-O(2)	1.865(16)	Cu(4)-O(8)	1.913(17)
W(1)-O(9)	1.893(17)	Cu(5)-O(18)	1.668(18)
W(2)-O(7)	1.864(17)	Cu(5)-O(10)	1.865(17)
W(2)-O(17)	1.877(15)	Cu(5)-O(14)	1.883(16)
W(2)-O(6)	1.907(15)	Cu(5)-O(15)	1.887(16)
W(3)-O(6)#1	1.875(17)	Cu(5)-O(16)	1.915(16)
W(3)-O(9)	1.882(17)	Cu(5)-O(19)	2.40(3)
W(3)-O(16)#1	1.902(16)	Cu(6)-O(12)	1.732(16)
W(3)-O(21)#1	2.41(2)	Cu(6)-O(17)	1.873(17)
W(3)-O(19)	2.46(3)	Cu(6)-O(3)	1.884(16)
W(4)-O(13)	1.698(16)	Cu(6)-O(2)#1	1.926(15)
W(4)-O(1)#1	1.905(18)	Cu(6)-O(1)	1.943(18)
W(6)-O(20)#1	2.496(18)	Cu(6)-Na(1)	3.555(13)
Cu(4)-O(13)	1.698(16)	Cu(1)-O(1A)	1.915(12)
Cu(4)-O(1)#1	1.905(18)	Cu(1)-N(5)	1.965(15)

Table S3 Bond angles (°) for **1**

O(5)-W(1)-O(8)	101.6(8)	W(2)-O(22)-W(6)	92.4(9)
O(5)-W(1)-O(2)	102.2(8)	C(18)-O(1A)-Cu(1)	134.2(13)
O(8)-W(1)-O(2)	87.7(7)	C(18)-O(2A)-Cu(3)	124.7(11)
O(5)-W(1)-O(9)	102.8(8)	C(38)-O(3A)-Cu(2)#3	135.0(13)
O(8)-W(1)-O(9)	155.6(9)	C(38)-O(4A)-Cu(7)	126.2(13)
O(2)-W(1)-O(9)	86.5(8)	C(5)-N(1)-C(1)	119.8(19)
O(5)-W(1)-O(8)	101.6(8)	C(5)-N(1)-Cu(3)	113.9(14)
O(5)-W(1)-O(2)	102.2(8)	C(1)-N(1)-Cu(3)	126.2(15)
O(8)-W(1)-O(2)	87.7(7)	N(3)-N(2)-C(6)	106.4(14)
O(11)-W(3)-O(6)#1	101.9(9)	N(3)-N(2)-Cu(3)	138.0(12)
O(11)-W(3)-O(9)	101.8(9)	C(6)-N(2)-Cu(3)	114.4(13)
O(6)#1-W(3)-O(9)	87.5(8)	N(2)-N(3)-C(8)	107.4(17)

O(11)-W(3)-O(16)#1	100.8(9)	N(2)-N(3)-Cu(1)#2	123.1(11)
O(6)#1-W(3)-O(16)#1	87.1(7)	C(8)-N(3)-Cu(1)#2	129.5(15)
O(9)-W(3)-O(16)#1	157.3(9)	C(13)-N(4)-C(9)	118.4(16)
O(11)-W(3)-O(6)#1	101.9(9)	C(13)-N(4)-Cu(1)	115.0(12)
O(11)-W(3)-O(9)	101.8(9)	C(9)-N(4)-Cu(1)	126.6(13)
O(1A)-Cu(1)-N(3)#2	89.5(6)	N(6)-N(5)-C(14)	111.2(15)
N(5)-Cu(1)-N(3)#2	97.6(6)	N(6)-N(5)-Cu(1)	135.2(11)
O(1A)-Cu(1)-N(4)	92.5(6)	C(14)-N(5)-Cu(1)	113.6(12)
N(5)-Cu(1)-N(4)	80.7(6)	N(5)-N(6)-C(16)	105.0(14)
N(3)#2-Cu(1)-N(4)	174.5(5)	N(5)-N(6)-Cu(3)#2	127.3(11)
N(9)-Cu(2)-O(3A)#3	90.8(6)	C(16)-N(6)-Cu(3)#2	127.8(12)
O(1A)-Cu(1)-N(3)#2	89.5(6)	N(1)-C(1)-C(2)	120(2)

Symmetry transformations used to generate equivalent atoms:
$^{\#1}$(-x+1,y,-z+3/2); $^{\#2}$(-x+1/2,-y+1/2,-z+1); $^{\#3}$(-x+1/2,-y+3/2,-z+1)

Table S4 Bond lengths (Å) for **2**

W(1)-O(8)	1.683(5)	Cu(1)-N(8)	1.973(6)
W(1)-O(5)	1.873(6)	Cu(1)-N(6)#4	1.978(6)
W(1)-O(6)#1	1.894(6)	Cu(1)-N(2)	1.995(6)
W(1)-O(4)	1.903(6)	Cu(1)-N(7)	2.078(6)
W(1)-O(6)	1.918(5)	Cu(1)-N(1)	2.355(6)
W(1)-O(2)	2.377(8)	Cu(2)-N(9)#4	1.944(6)
W(1)-O(1)#2	2.413(7)	Cu(2)-N(5)	1.964(6)
Si(1)-O(1)#2	1.601(14)	Cu(2)-N(3)	2.012(6)
Si(1)-O(2)#5	1.625(9)	Cu(2)-N(4)	2.024(6)
Si(1)-O(1)#2	1.601(14)	Cu(2)-O(1W)	2.231(5)

Table S5 Bond angles (°) for **2**

O(8)-W(1)-O(5)	100.6(3)	O(1)-Si(1)-O(2)#5	70.1(3)
O(8)-W(1)-O(6)#1	100.0(3)	O(1)#2-Si(1)-O(2)#5	109.9(3)
O(5)-W(1)-O(6)#1	89.0(3)	O(1)-Si(1)-O(2)#6	109.9(3)
O(8)-W(1)-O(4)	100.4(3)	O(1)#2-Si(1)-O(2)#6	70.1(3)
O(5)-W(1)-O(4)	90.2(2)	O(2)#5-Si(1)-O(2)#6	180.0(7)
O(6)#1-W(1)-O(4)	159.3(3)	O(1)-Si(1)-O(2)#1	109.9(3)
O(8)-W(1)-O(6)	100.2(3)	O(1)#2-Si(1)-O(2)#1	70.1(3)
O(5)-W(1)-O(6)	159.2(3)	O(2)#5-Si(1)-O(2)#1	71.0(3)
O(6)#1-W(1)-O(6)	87.4(3)	O(2)#6-Si(1)-O(2)#1	109.0(3)
O(4)-W(1)-O(6)	86.0(3)	O(1)-Si(1)-O(2)#3	70.1(3)
O(8)-W(1)-O(2)	158.1(3)	O(1)#2-Si(1)-O(2)#3	109.9(3)
O(5)-W(1)-O(2)	65.0(3)	O(2)#5-Si(1)-O(2)#3	109.1(3)
O(6)#1-W(1)-O(2)	96.3(3)	O(2)#6-Si(1)-O(2)#3	70.9(3)
O(4)-W(1)-O(2)	64.8(3)	O(2)#1-Si(1)-O(2)#3	180.0

O(6)-W(1)-O(2)	95.0(3)	O(1)-Si(1)-O(2)#2	70.1(3)
O(8)-W(1)-O(1)#2	156.4(3)	O(1)#2-Si(1)-O(2)#2	109.9(3)
O(5)-W(1)-O(1)#2	96.5(3)	O(2)#5-Si(1)-O(2)#2	109.1(3)
O(6)#1-W(1)-O(1)#2	63.9(3)	O(2)#6-Si(1)-O(2)#2	70.9(3)
O(4)-W(1)-O(1)#2	95.6(3)	O(2)#1-Si(1)-O(2)#2	71.0(3)
O(6)-W(1)-O(1)#2	63.6(3)	O(2)#3-Si(1)-O(2)#2	109.0(3)
O(2)-W(1)-O(1)#2	45.5(4)	O(1)-Si(1)-O(2)	109.9(3)
O(3)-W(2)-O(4)	100.4(3)	O(1)#2-Si(1)-O(2)	70.1(3)
O(3)-W(2)-O(7)	101.0(3)	C(16)-N(6)-Cu(1)#4	128.3(5)

Symmetry transformations used to generate equivalent atoms:
$^{\#1}$(-y+1,x-y,z); $^{\#2}$(-x+4/3,-y+2/3,-z+2/3); $^{\#3}$(y+1/3,-x+y+2/3,-z+2/3); $^{\#4}$(-x+5/3,-y+4/3,-z+4/3); $^{\#5}$(x-y+1/3,x-1/3,-z+2/3); $^{\#6}$(-x+y+1,-x+1,z)

Table S6 Comparison of literature results of various POM-based catalysts used in photocatalytic H_2 evolution

Catalyst	**Photosensitizer**	**Sacrificial agent**	**Activity ($\mu mol\ g^{-1}h^{-1}$)**	**Ref.**
$[Cu_2(bim)_4(H_2O)_2](HBW_{12}O_{40})_2\cdot(H_2bim)_2\cdot 8H_2O$	$[Ir(dtbbpy)(ppy)_2][PF_6]$	TEOA	13025	1
$[Cu_2(bim)_4(H_2O)_2](H_3PW_{10}Ti_2O_{40})_2\cdot(H_2bim)_2\cdot 8H_2O$	$[Ir(dtbbpy)(ppy)_2][PF_6]$	TEOA	17075	1
$[Cu(C_8H_7N_3)(H_2O)_2]_2[(C_6H_5PO_3)_2Mo_5O_{15}]\cdot 4H_2O$	$[Ir(dtbbpy)(ppy)_2][PF_6]$	TEOA	4423	2
$[Cu(phen)(H_2O)][Cu(phen)(H_2O)_2][(C_6H_5PO_3)_2Mo_5O_{15}]\cdot 2H_2O$	$[Ir(dtbbpy)(ppy)_2][PF_6]$	TEOA	6399	2
$[Cu^{II}_2(bibe)(pzta)_2][H_2Mo_8O_{26}]$	$[Ir(dtbbpy)(ppy)_2][PF_6]$	TEA	330	3
$[Cu(dap)_2]_2[\{Cu_8(dap)_4(H_2O)_2\}(SiW_9O_{34})_2]\cdot 7H_2O$	$[Ir(dtbbpy)(ppy)_2][PF_6]$	TEOA	547	4
$[Cu(dap)_2(H_2O)]_2[Cu(dap)_2]_2[\{Cu_6(dap)_2\}(SiW_9O_{34})_2]\cdot 8H_2O$	$[Ir(dtbbpy)(ppy)_2][PF_6]$	TEOA	508	4
1	$[Ir(dtbbpy)(ppy)_2][PF_6]$	TEOA	16831	This work
2	$[Ir(dtbbpy)(ppy)_2][PF_6]$	TEOA	11041	This work

(1) Y. H. Zhu, Z. Y. Du, J. L. Wang, J. B. Yang, H. Mei and Y. Xu, *Inorg. Chem.*, 2022, **61**, 20397-20404.
(2) H. Xu, Q. Chen, J. L. Wang, Q. Wang, C. Y. Jiao, P. F. Yan, H. Mei and Y. Xu, *Inorg. Chem.*, 2023, **62**, 18878-18886.

(3) C. J. Zhang, X. Liu, G. N. Cui, L. M. Dong, F. Y. Sui and H. J. Pang, *J. Mol. Struct.,* 2022, **1262**, 132995.
(4) Z. M. Su, M. Zhang, Q. Q. An, D. Qin, H. L. Li, H. J. Lv, Z. Y. Jia, Q. Zhang and G. Y. Yang, *New J. Chem.,* 2020, **44**, 11035.